International Journal of Multimedia and Ubiquitous Engineering
Vol.11, No.7 (2016), pp.219-234
http://dx.doi.org/10.14257/ijmue.2016.11.7.22

Nonsubsampled Contourlet Transform Based Infrared Image Super-Resolution by Using Sparse Dictionary and Residual Dictionary

Kangli Li[1], Wei Wu[1,*], Xiaomin Yang[1], Yingying Zhang[1], Binyu Yan[1], Wei Lu[2] and Gwanggil Jeon[3]

[1]*School of Electronics and Information Engineering, Sichuan University, Chengdu, Sichuan, 610064 P.R.China*
[2] *School of software Engineering, Beijing Jiaotong University, Beijing 100044, P.R .China*
[3]*Department of Embedded Systems Engineering, University of Incheon, 12-1 Songdo-dong, Yeonsu-gu, Incheon406-772, Republic of Korea*
likangli0902@163.com; { wuwei, arielyang}@scu.edu.cn; zhangyinyingwei@sina.com; yby@scu.edu.cn ;gjeon@inu.ac.kr

Abstract

Due to the limitation of hardware, Infrared (IR) image has low-resolution (LR) and poor visual quality. To enhance the Infrared image's resolution, super-resolution (SR) is a good solution. However, the conventional SR methods have some drawbacks. Firstly, the trained dictionary is an unstructured dictionary, which may lead to worse results. Secondly, the representation of the image is too simple to effectively represent image. Finally, only one high-resolution (HR)-LR dictionary pair is adopted to infer HR IR image. However one HR-LR dictionary pair is not good enough to obtain good results. To resolve these problems, in this paper, firstly, the sparse dictionary is introduced into the IR image SR to get better results. Secondly, nonsubsampled contourlet transform (NSCT) is employed to obtain a better representation of IR image. Finally, to achieve better r-esults, two HR–LR sparse dictionary pairs, which consists of a primitive sparse dictionary pair and a residual sparse dictionary pair, instead of one HR-LR dictionary pair are adopted. The experiment results indicate that the subjective visual effect and objective evaluation acquire excellent performance in the proposed method. Besides, this method is superior to other methods.

Keywords*: Infrared Images, Super-Resolution, Dictionary Learning, Sparse representation, Nonsubsampled Contourlet Transform (NSCT)*

1. Introduction

Infrared (IR) thermal-imaging cameras can generate infrared images, which would not be affected by visible light, through thermal radiation of the scene. Therefore, the IR i-mage can be applied to security surveillance, biomedical applications, military, *etc.* H-owever, due to the limitation of hardware, the resolution of infrared image is very low. These low-resolution (LR) IR images may lead to a failure for further analysis.

Super-resolution (SR) method is a technique, which is to reconstruct a high-resolution (HR) image through a single LR image or multiple LR images. And the SR method is one of the best solutions for improving resolution of LR IR image. There are many SR methods, including interpolation method [1-3] reconstruction based SR [4-8] and learning-based SR method [9-15]. Generally, a SR image by using interpolation method

*Corresponding Author

ISSN: 1975-0080 IJMUE

lacks more high-frequency details, has highly blurred edges and many undesired artifacts. In the reconstruction based SR method, to reconstruct a HR image it needs a sequence of LR images of the same scene. And reconstruction based SR method is limited by its low magnification. In the learning-based SR method, the HR image is generated from its corresponding LR image with a training set, which contains LR and HR image pairs. Freeman *et al* proposed the method that training Markov network to find the relationship between LR image patches and their corresponding HR image patches [16]. Zeyde *et al* proposed to upscale image sparse representation modeling [17]. Though these methods have a good performance, the complexity is very high and they need a lot of memory.

Until now, there are few researches of IR images SR. Yu *et al* proposed an algorithm that based on non-local means and steering kernel regression [18]. Zhao *et al* propose a SR method combined with nonsampled contourlet transform (NSCT) and parabolic error edge preserving interpolation [19]. Wang *et al* consider the performance of a robust super-resolution on simulated infrared images [20]. Liu *et al* [21] proposed an IR image SR method via group sparse representation, and got a dictionary pair that was jointly trained through combining method of group orthogonal matching pursuit and the K-SVD [22].

Although the above mentioned methods have good performance, they have several drawbacks. Firstly, the trained dictionary is an unstructured dictionary. This may lead to worse results. Besides, the derivatives filters are adopted to extract image features. However, those features are too simple to effectively represent image. Finally, only one HR-LR dictionary pair is adopted to infer HR IR image. However one HR-LR dictionary pair is not good enough to obtain good results.

To resolve these problems, firstly, the sparse dictionary is introduced into the IR image SR to solve the problem that the trained dictionary is an unstructured dictionary. The sparse dictionary is based on a sparsity model of the dictionary atoms over a base dictionary. NSCT is fully shift-invariance, multi-scale and multi-direction, so that it can enrich IR image feature, avoid the frequency aliasing, and preserve the edge information perfectly. Therefore, NSCT is employed in the proposed method to overcome the problem that the derivatives filters are too simple to effectively represent image. Finally, two HR-LR sparse dictionary pairs, which consists of a primitive sparse dictionary pair and a residual sparse dictionary pair, are adopted in this paper. It can solve the problem that one HR-LR dictionary pair is not good enough to obtain good results. The primitive estimated HR IR image is first inferred with primitive sparse dictionary pair. Subsequently, a similar process is applied to the primitive estimated result with residual sparse dictionary pair. With the two sparse dictionary pairs, better results can be achieved.

The remainder of this paper is organized as follow. Section 2 reviews the NSCT decomposition. Section 3 presents the details of our proposed method. Section 4 shows the experimental results and make a comparison with other related SR reconstruction methods. Section 5 summarizes this paper.

2. Nonsampled Contourlet Transform Theory

Contourlet transform (CT) has been recently introduced, and has been widely used in image recognition, image denoising, and image enhancement [23]. The CT employs the Laplacian pyramid (LP) and directional filter bank (DFB) to obtain the multi-scale decomposition and directional decomposition respectively. The contourlet transform could sparsely represent a natural image, and has the ability to capture the contour information in all directions and all scales. Compared with wavelet transform, contourlet transform is a real 2D discrete transform. Because of the downsampling and upsampling in LP and DFB, the contourlet transform faces lack of shift-invariance.

To overcome this problem, Cunha *et al* proposed NSCT, which is a shift-variant version of the CT [24]. The NSCT [25-29] eliminates the downsamplers and upsamplers

during the decomposition and the reconstruction of the image to avoid the frequency aliasing of the CT and achieve the shift-invariance. NSCT consists of two filter banks: nonsubsampled pyramid (NSP) and nonsubsampled directional filter bank (NSDFB) as show in Figure 1, NSP decomposes the input image into a high-frequency subband and a low-frequency subband at each NSP decomposition level, NSDFB decomposes the high-frequency subband into a few directional subbands. After n levels decomposition, NSP can result in one low-frequency image and n high-frequency images having the same size as the input image. It is NSDFB that allows the direction decomposition with k stages in high-frequency images from NSP at each scale. And $2k$ directional sub-images, which have the same size as the input image, can be obtained during this process. As a result, there would be one low-frequency image and $\sum_{i=1}^{n} 2^{k_i}$ high-frequency images, where k_i denotes the number of direction for scale i. NSCT is adopted in this paper, since NSCT has good characteristic of shift-invariant, multi-scale, and multi-direction.

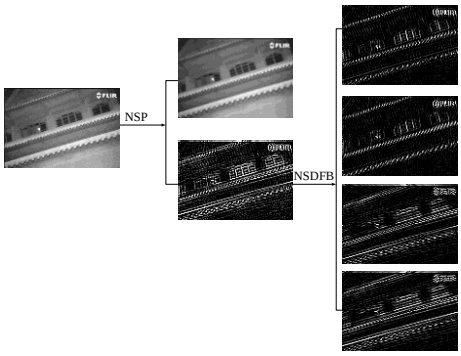

Figure 1. Schematic Diagram of NSCT

3. Infrared Image Super-Resolution Based on Sparse Dictionary and NSCT

The framework of the proposed method is shown in Figure 2. The proposed method consists of two stages: the training stage and the testing stage. In the training stage, two HR - LR sparse dictionary pairs are obtained from the training image set. In the testing stage, input LR IR image is super resolved to generate a HR IR image with the help of the two HR - LR sparse dictionary pairs obtained in training stage.

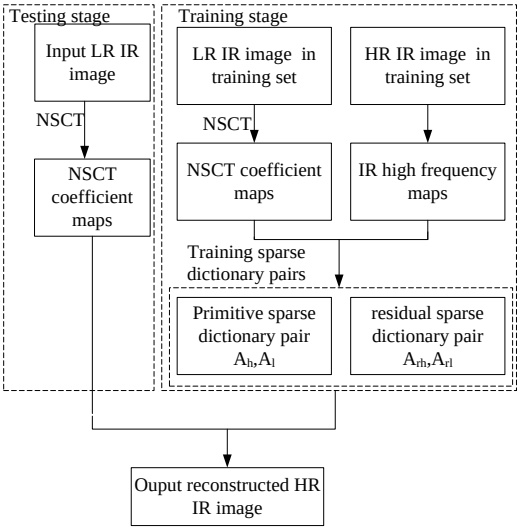

Figure 2. Flowchart of the Proposed Algorithm

3.1. Sparse Dictionary

Over-complete dictionaries have been used in image process. However, their atoms used in the dictionaries have some underlying sparse structure over more fundamental dictionary. The conventional over-complete dictionary can be formulated as the following optimization problem:

$$\min_{D,\phi} \left\| B - D\phi \right\|_F^2 \quad s.t \quad \forall i \left\| \phi_i \right\| \le t, \forall j \left\| d_j \right\| = 1 \tag{1}$$

where B is an image block, the coefficient vector ϕ is the sparse representation of B. t is the sparse tolerance of ϕ_i. However, the dictionary generated in this way is unstructured [30]. This may lead to worse results. To overcome this problem, sparse dictionary is introduced in this paper. The dictionary D has a sparse representation over a basic dictionary. Specifically, this dictionary is composed of two parts: base dictionary and sparse matrix representation.

The sparse dictionary can be expressed as:

$$D = \eta \times C \tag{2}$$

where η is a base dictionary with good regularity. C is an atom representation matrix with good flexibility. Over-complete DCT dictionary, Wavelet dictionary and so on can be used as a base dictionary. In this paper, we chose over-complete DCT dictionary as the base dictionary. Thus sparse dictionary can be calculated as Eq. (3):

$$\min_{C,\phi} \left\| B - \eta C\phi \right\|_F^2 \quad s.t \quad \begin{cases} \forall i \left\| \phi_i \right\|_0 \le t \\ \forall j \left\| c_j \right\|_0 \le s \end{cases}, \left\| \eta c_j \right\|_2 = 1 \tag{3}$$

where B is an image block, ϕ is the sparse representation matrix of B, t and s is the sparse tolerance of ϕ and C, respectively.

The task of obtaining sparse dictionary can be divided into two procedures: 1) sparse-coding the image block in B; 2) updating the dictionary atoms. In the stage of solving sparse representation, we can use arbitrary signal sparse decomposition approach. In this paper, we use OMP [31] for sparse-coding and sparse K-SVD algorithm for the dictionary training. In the phase of updating the dictionary atoms, every time we only update one

atom, *i.e.*, keep other atoms fixed to solve the optimal solution for the target equation. In this paper, we exploit the sparse KSVD to solve the Eq. (3).

3.2. Training Stage

Primitive HR-LR sparse dictionary pair is learned to reconstruct primitive HR IR image from a single LR IR image input. There are some gaps between the reconstructed primitive HR IR image and its corresponding reference HR IR image. For convenience, the difference between reconstructed HR IR image and the reference HR IR image can be called residual IR image. To get a better result, we need to estimate the residual IR image with residual sparse dictionary. Therefore, residual HR-LR sparse dictionary pair is introduced into this paper to reconstruct the residual IR image. The process of sparse dictionary learning is described in Figure 3.

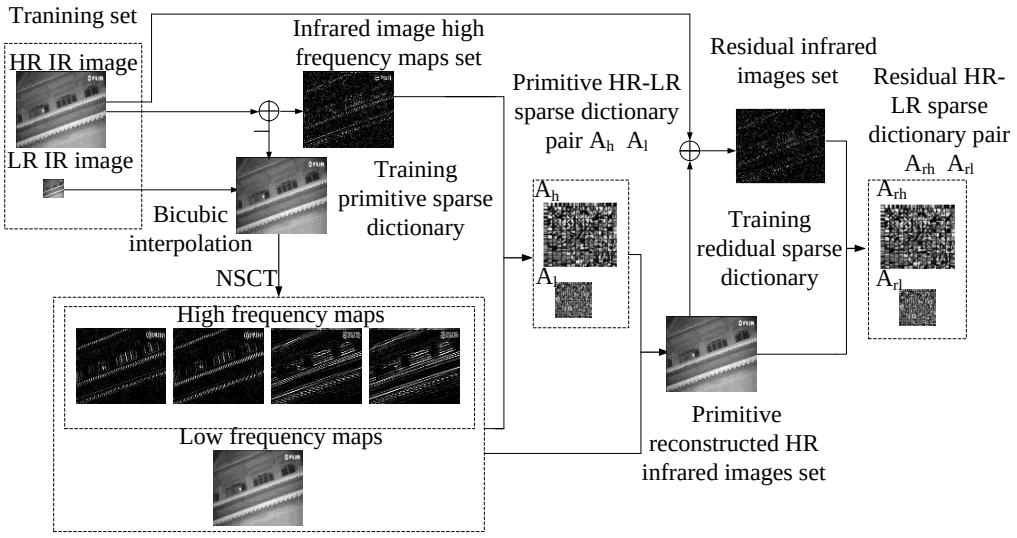

Figure 3. The Framework of the Sparse Dictionary Training Process

The framework of the sparse dictionary training process is given in Figure 3. The steps of the sparse dictionary training process are as follows:

1) Firstly, the input LR IR images I_l^m are enlarged to yield enlarged image $I_{l'}^m, m = 1, 2, ..., \mathrm{M}$ with the Bicubic interpolation. Then, we obtain the differences between the HR IR images and their corresponding LR IR images, namely IR image high frequency map I_{hf}^m [32].

2) We perform NSCT to decompose each $I_{l'}^m$ image into a one-level pyramid. After that, we can get one low frequency map $C_{llf'}^m$ and four high frequency maps $C_{lhf1'}^m, C_{lhf2'}^m, C_{lhf3'}^m, C_{lhf4'}^m$, we use the Difference of Gaussian (DoG) filter to extract the detail information from the low frequency map as the feature vector map. $C_{llf'}^m$ The five maps $C_{llf'}^m, C_{lhf1'}^m, C_{lhf2'}^m, C_{lhf3'}^m, C_{lhf4'}^m$ are divided into blocks to build a NSCT coefficient block structure database $B = \left\{ b_l^{mk} \right\}$. We take overlapping blocks with the size of $n \times n$ from the five maps $C_{llf'}^m, C_{lhf1'}^m, C_{lhf2'}^m, C_{lhf3'}^m, C_{lhf4'}^m$. Then, we transform all the blocks into vectors

as $b_{llf'}^{mk}, b_{lhf1'}^{mk}, b_{lhf2'}^{mk}, b_{lhf3'}^{mk}, b_{lhf4'}^{mk}, k = 1, 2, ...K$, and integrate those vectors from different map to build a feature vector b_l^{mk}, K is the total number of blocks in a map. The framework of generate feature vector as follow Figure 4. And the high frequency map I_{hf}^m is divided into blocks $B = \{b_h^{mk}\}$ with $n \times n$ pixels overlap.

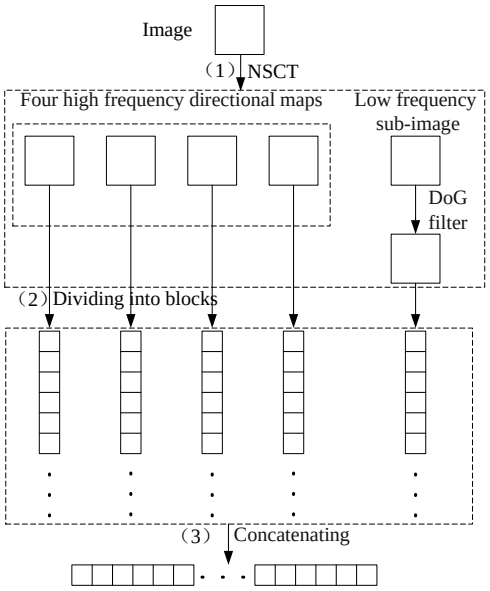

Figure 4. The Framework of Generate Feature Vector. (1) NSCT is applied to Decompose Input Image into one Level, (2) All Images are Divided into Blocks with $n \times n$ Pixels Overlap, (3) All the Blocks are Concatenated into a Feature Vector

3) Through the Eq. (4), we can obtain the primitive LR sparse dictionary C_l and the sparse representation ϕ.

$$\min_{C_l, \phi} \left\| b_l^k - \eta C_l \phi \right\|_2^2 \quad s.t \quad \forall i \left\| \phi_i \right\|_0 \le t, \left\| c_{lj} \right\|_2 \le s, \left\| \eta c_{lj} \right\|_2 = 1 \tag{4}$$

where η is a DCT basic dictionary, ϕ is the sparse representation of b_l^k, t is the signal sparsity threshold, s is the atom sparsity threshold. After that, we acquire LR sparse dictionary C_l, and can calculate primitive HR sparse dictionary from the HR image blocks by $\eta C_h = b_h^k \phi^T (\phi \phi^T)^{-1}$.

4) Finally, we can recover the enlarged LR images $I_{l'}^m$ by using the primitive sparse dictionary pair C_l and C_h, then we get the primitive reconstruction IR image I_{ho}. In the next subsection, we will explain the details of the reconstruction method. The differences between the HR reference images and the primitive HR IR images are the residual IR images. The residual sparse HR-LR dictionary pair C_{rh}、C_{rl} can be trained with the primitive HR IR image and the residual IR image. Then we use the sparse dictionary

learning method as mentioned in previous step to get the residual sparse HR-LR dictionary pair C_{rh}、 C_{rl}.

3.3. Super-Resolution Image Reconstruction

For a HR IR image block, it can be represented as $b_h^k = \eta C_h \alpha_i$. Because the LR IR image block and the HR IR image block have the same sparse representation, the problem of finding the sparse representation α_i of LR IR image block can be presented as:

$$\min_{\alpha_i} \|\alpha_i\|_0 \quad s.t \quad \left\| b_l^k{}_i - F\eta C_l \alpha \right\|_2^2 \le \lambda \tag{5}$$

where F is a feature extraction operation. λ is the tolerance degree of error. The optimization problem (5) is NP-hard. However, we can use the minimizing the l^1 norm to solve the problem, as follow:

$$\min_{\alpha_i} \|\alpha_i\|_1 \quad s.t \quad \left\| b_l^k - F\eta C_l \alpha_i \right\|_2^2 \le \lambda \tag{6}$$

Using OMP, sparse representation α_i can be obtained.

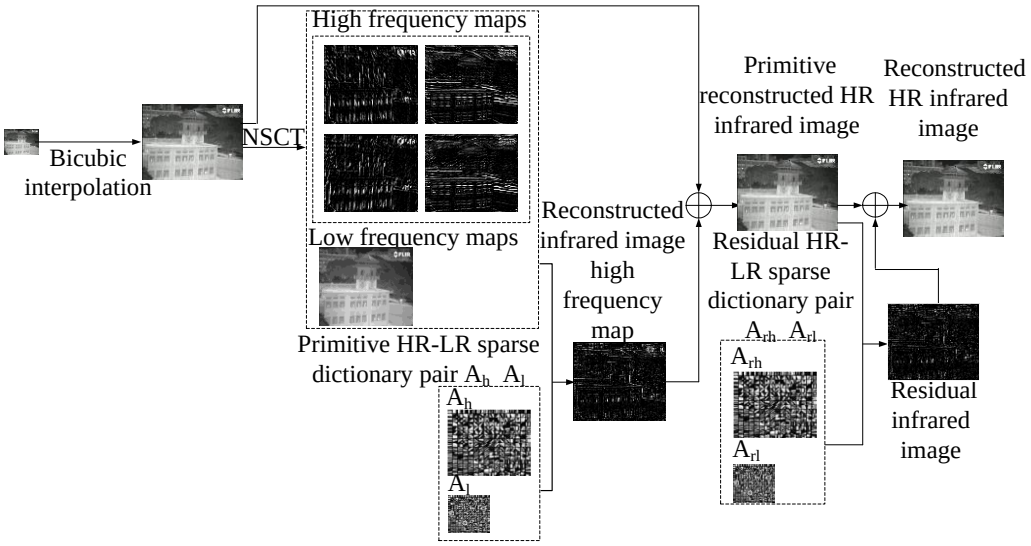

Figure 5. The Framework of the Testing Process

The details of the testing process show in Figure 5, go through the steps as follows:

(1) Firstly, the input LR IR images I_{TI} are enlarged to yield enlarged image $I_{TI'}$ with the Bicubic interpolation. Then, we can obtain the NSCT coefficient blocks of the LR IR image $B = \{b_l^k\}\ k = 1, 2, ...K$ by using the same feature extraction method in the training stage.

(2) Subsequently, we obtain the sparse representation $\{\alpha_i\}$ of the NSCT coefficient blocks $B = \{b_l^k\}\ k = 1, 2, ...K$ by using OMP through Eq.(6). Then using $b_h^{k*} = \eta C_h \alpha_i$, we can get the high frequency blocks of IR image. The estimated high frequency blocks are merged to create the primitive high frequency map I_{fh}^*.

(3) Then, we integrate the enlarged image $I_{Tl'}$ with the primitive high frequency map I_{fh}^{*} to obtain the primitive reconstructed HR IR image I_{ho}.

(4) Similarly, we can reconstruct residual IR image I_r with residual sparse HR-LR dictionary pair C_{rh}、C_{rl}.

(5) Finally, we obtain the HR IR image I_h by integrating the primitive reconstructed HR IR image I_{ho} and the reconstruct residual IR image I_r.

4. Experimental Results and Discussion

4.1. Comparison of Different Method

In this section, we compare our method with other methods such as Bicubic interpolation, nearest neighbor interpolation, Yang's method, KSVD method, and Zhang's method [33]. The IR images used in our experiment consist of two categories, *i.e*. face images, natural scene images. The face images are from USTC-NVIE database [34], while the natural scene images are captured by ourselves. The FLIR Tau 320[35] is adopted to capture the natural scene images.

For IR face images, we select fifty HR IR images, which have the same size 228×300.The training images randomly select thirty-four from the fifty HR IR images and the rest sixteen HR IR images are used as inputs for testing. For natural scene IR images, we pick up seventy–five HR IR images. The IR images are organized into two parts: training samples and test samples .The training samples include sixty- two IR images while the testing samples include thirteen IR images. The natural scene IR images are with the same size 240×348. The HR IR images are downsampled by factor of 3 to constitute the LR IR images. Some of the training images are shown in Figure 6 and Figure 7.

In our experiments, we use patches of size 9×9 for NSCT coefficient maps and HR IR image. And these patches overlap 3 pixels between adjacent blocks. In each experiment, the size of sparse dictionary is 1024. And we divide the images into one level, which have four directions. We use the DoG filter to extract the detail information from the low frequency map as the feature vector map. We evaluate the results of various methods by both visually and qualitatively in peak signal-to-noise ratio (PSNR) and the structural similarity measurement (SSIM).

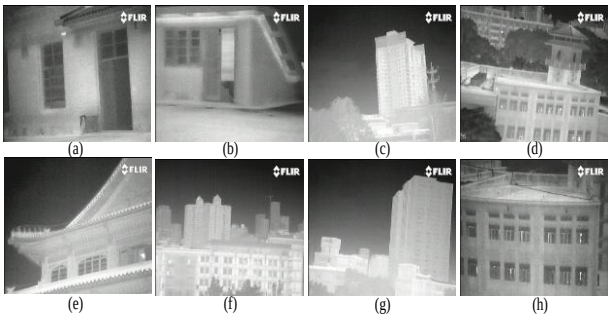

Figure 6. Training IR Images with Natural Scene

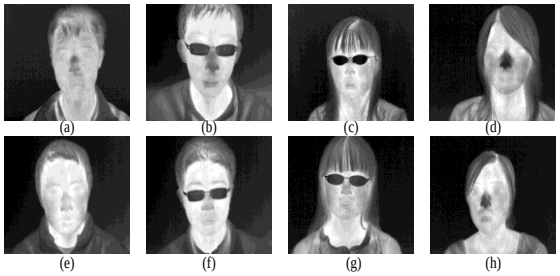

Figure 7. Training IR Images with Face

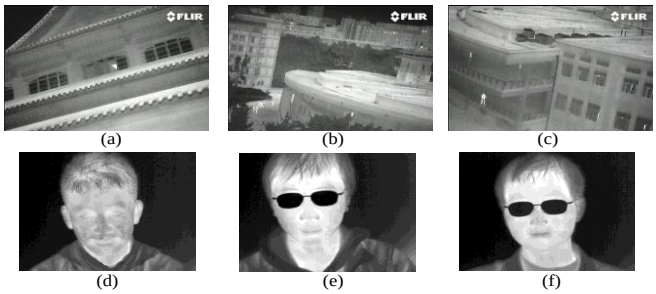

Figure 8. Part of the Testing IR Images. (a) A Building a IR Image, (b) a Building B IR Image, (c) A Building C IR Image, (d) A Face a IR Image, (e) A Face B IR Image, (f) A Face C IR Image

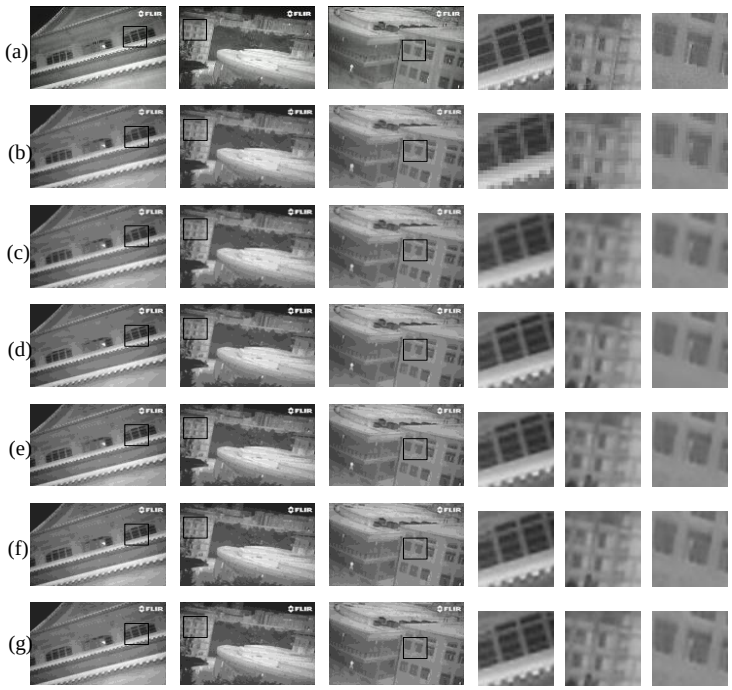

Figure 9. Experimental Results with Images. (a) Reference HR Image, (b) Results Obtained with Nearest Neighbor, (c) Results Obtained with Bicubic Interpolation, (d) Results Obtained with Yang's Method, (e) Results Obtained with K-SVD Method, (f) Results Obtained with Zhang's Method, (g) Results Obtained with the Proposed Method

Figure 10. Experimental Results with Images. (a) Reference HR Image, (b) Results Obtained with Nearest Neighbor, (c) Results Obtained With Bicubic Interpolation, (d) Results Obtained with Yang's Method, (e) Results Obtained with K-SVD Method, (f) Results Obtained with Zhang's Method, (g) Results Obtained with the Proposed Method

Figure 9 (a) and Figure 10 (a) are the original IR images for natural scene images and face images respectively. Figure 9(b-g) and Figure 10 (b-g) are the reconstructed IR images by nearest neighbor interpolation, Bicubic interpolation, Yang's method, KSVD method, Zhang's method and the proposed method respectively. Three columns on the right in Figure 9(a-g) and Figure 10(a-g) are the zoomed up version of the marked regions in the images in the three columns on the light respectively, where the details of the results of the proposed methods can be observed. From Figure 9(b) to (c) and Figure 10(b) to (c), we can see that the reconstruction results lack high frequency component, have no image details, and get blurred edges. While the reconstruction results of Yang's, KSVD, Zhang's and the proposed method is relatively clear. The reconstruction image of the Yang's, KSVD, Zhang's and proposed method can restored the image details. Besides, the reconstruction of image edge texture by KSVD method has improved compared with Yang's method. From Figure 9-10, we can find that the proposed algorithm is the best effect and the recovered image details are most similar to the reference HR IR image.

Table 1. Performance Comparison Table

Image	Evaluation index	Nearest	Bicubic	Yang's method	KSVD method	Zhang's method	Our method
building A	PSNR	25.501	26.563	27.305	27.815	27.766	**27.824**
	SSIM	0.729	0.765	0.775	0.800	0.799	**0.800**
building B	PSNR	25.018	25.786	26.414	26.832	26.829	**26.855**
	SSIM	0.701	0.735	0.752	0.774	0.774	**0.777**
building C	PSNR	26.878	27.515	27.997	28.392	28.418	**28.440**
	SSIM	0.735	0.763	0.770	0.791	0.792	**0.794**

face A	PSNR	31.100	35.433	35.731	36.408	36.387	**36.601**
	SSIM	0.868	0.907	0.903	0.915	0.915	**0.917**
face B	PSNR	29.470	33.354	34.781	35.735	35.734	**35.846**
	SSIM	0.863	0.905	0.901	0.916	0.915	**0.917**
face C	PSNR	30.200	33.954	35.355	36.276	36.608	**36.673**
	SSIM	0.881	0.919	0.912	0.928	0.928	**0.928**

The Table 1 indicates that our method achieves the highest PSNR and SSIM, which f-urther demonstrates that our method is superior to other methods.

4.2. Parameter Analysis

In this section, we investigate the impacts of the parameters on the results. The main p-arameters of the proposed method consist of four parameters, *i.e.*, the level of the number of NSCT, the number of directions of NSCT, the sparse dictionary size and the low frequency feature extraction methods.

Figure 13 shows the impact of the level number of NSCT on the results. From Figure 13 we can see that one level is the best results. With the increase of the level number, the result is getting worse. The reason of the phenomenon may be that the noise would be introduced when level number increases.

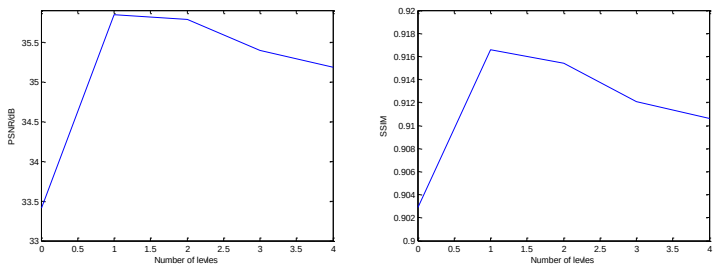

(a) (b)

Figure 13. Impact on SR Quality of the Number of Level of NSCT. (a) The PSNR under Different Numbers of Levels of NSCT, (b) The SSIM under Different Numbers of Levels of NSCT

Figure14 shows the impact of the directional number on the results. When the first level only has one direction, the PSNR and SSIM is the lowest. With the increase of the directional number, The PSNR and SSIM would increase gradually. When the number of direction increased to a certain degree, the PSNR and SSIM tend to be stable. With the increase of the number of directions, the performance of the proposed method would become better.

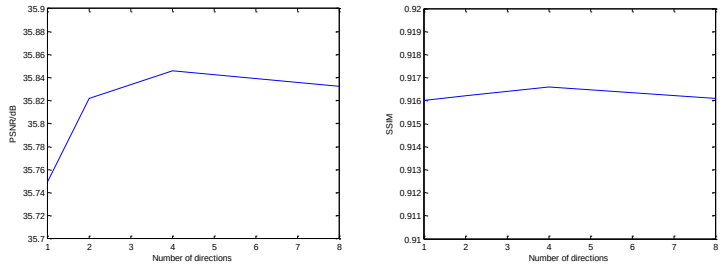

(a) (b)

Figure 14. Impact on SR Quality of the Number of Directions of NSCT. (a) The PSNR Under Different Numbers of Directions of NSCT, (b) The SSIM under Different Numbers of Directions of NSCT

Figure 15 shows the impact of the sparse dictionary size on the results. We train our dictionaries of size 256, 512, 1024, and 1200, and apply them to the same input images. From Figure 15, we find that when the sparse dictionary size increases, the PSNR and SSIM tend to rise slowly. Thus, we have a conclusion that the larger the sparse dictionary size is, the better SR results gain.

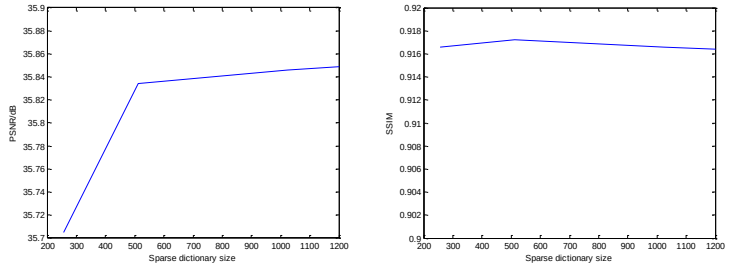

(a) (b)

Figure 15. Impact on SR Quality of Size of Sparse Dictionary. (a) The PSNR under Different Sparse Dictionary Size, (b) The SSIM under Different Sparse Dictionary Size

Figure 16 shows the impact of the feature extraction method for the low frequency map on the results. The phase congruency filter [36], Gabor filter [37], Gradient filter [12], DoG filter [32] are used to extract the feature of low frequency map respectively. From the Figure 16 we can observe that the DoG filter is the best one.

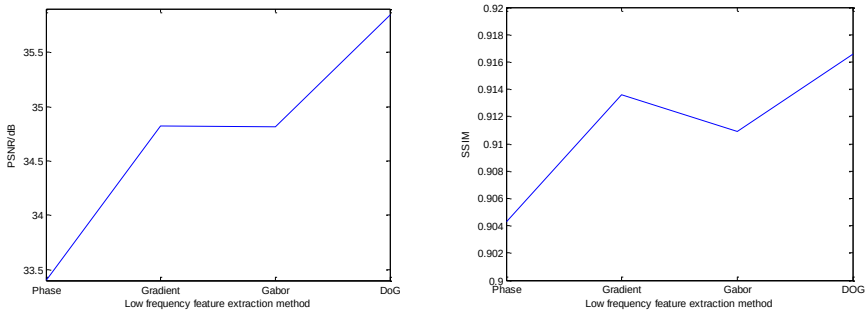

(a) (b)

Figure 16. Impact on SR Quality of Low- Frequency Feature Extraction Method. (a) The PSNR under Different Method about Feature Extracted, (b) The SSIM under Different Methods about Feature Extracted

5. Conclusion

In this paper, sparse representation is applied to solve the SR problem of IR image, which is based on NSCT and sparse dictionary. Compared with the conventional dictionaries, the sparse dictionary has regularity and adaptively. Furthermore, compared with conventional SR methods, two sparse dictionary pairs are proposed in this paper. The primitive sparse dictionary pair is learned to reconstruct primitive HR IR image, but it loses some details compare with the corresponding reference HR image completely. Therefore, residual sparse dictionary pair is learned to reconstruct residual information. The conventional extracted feature method that extract the gradient maps, but it can't fully applied the image features. In this paper, we use the NSCT to extract the feature. Because the NSCT is multi-scale, multi-direction, translation invariance, it enriches the image feature and avoids aliasing. The experimental results show that the proposed method performs better than other methods.

Acknowledgments

The research is sponsored by the National Natural Science Foundation of China (No. 61271330 and No. 61411140248), the Science and Technology Plan of Sichuan Province (No. 2014GZ0005), the Scientific Research Foundation for the Returned Overseas Chinese Scholars, State Education Ministry, the National Science Foundation for Postdoctoral Scientists of China (No. 2014M552357), and the Research Fund for the Doctoral Program of Higher Education (No. 20130181120005).

References

[1] [2]L. Zhang and X. Wu, "An Edge-Guided Image Interpolation Algorithm via Directional Filtering and Data Fusion", IEEE Transaction on Image Processing, vol. 15, no. 8, **(2006)**, pp. 2226-2238.
[2] X. Zhang and X. Wu, "Image Interpolation by Adaptive 2-D Autogressive Modeling and Soft Decision Estimation", IEEE Transaction on Image Processing, vol.17, no. 6, **(2008)**, pp. 887-896.
[3] K. Guo, X. Yang, H. Zha, W. Lin and S. Yu, "Multiscale Semilocal Interpolation with Antialiasing", IEEE Transaction on Image Processing, vol. 21, no. 2, **(2012)**, pp. 615-625.
[4] J. D. V. Ouwerkerk, "Image super-resolution survey", Image and Vision Computing, vol. 24, no. 10, **(2006)**, pp. 1039-1052.
[5] S. P. Kim, N. K. Bose and H. M. Valenzuela, "Recursive Reconstruction of High-Resolution Image from Noisy Under sampled Multiframes", IEEE Transactions on Acoustics, Speech and Signal Processing, vol. 38, no. 6, **(1990)**, pp. 1013-1027.
[6] P. Vandewalle, S. Susstrunk and M. Vetterli, "A Frequency Domain Approach to Registration of Aliased Images with Application to Super-resolution", EURASIP Journal on Applied Signal Processing, **(2006)**, pp. 1-14.
[7] H. Stark and E. Oskoui, "High-resolution image recovery from image-plane arrays using Convex Projections", Journal of the Optical Society of America A, vol. 6, no. 11, **(1989)**, pp. 1715-1726.
[8] A. J. Patti, M. I. Sezan and A. M. Tekalp, "Superresolution Video Reconstruction with Arbitrary Sampling Lattices and Nonzero Aperture Time", IEEE Transactions on Image Processing, vol. 6, no. 8, **(1997)**, pp. 1064-1076.
[9] S. Baker and T. Kanade, "Limits on Super-Resolution and How to Break Them", IEEE Transaction on Pattern Analysis and Machine Intelligence, vol. 24, no. 9, **(2002)**, pp. 1167-1183.
[10] [1]W. T. Freeman, T. R. Jones and E. C. Pasztor, "Example-Based Super-Resolution", IEEE Computer Graphics and Applications, vol. 22, no. 2, **(2002)**, pp. 56-65.
[11] J. Yang, J. Wright, Y. Ma and T. Huang, "Image Super-Resolution as Sparse Representation of Raw Image Patches", IEEE Conference on Computer Vision and Pattern Recognition, CVPR, Anchorage, AK, **(2008)**, pp.1-8.
[12] J. Yang, J. Wright, T. Huang and Y. Ma, "Image Super-Resolution via Sparse Representation", IEEE Transaction on Image Processing, vol. 19, no. 11, **(2010)**, pp. 2861-2873.
[13] [1]W. Dong, L. Zhang, R. Lukac, and G. Shi, "Sparse Representation Based Image Interpolation With Nonlocal Autoregressive Modeling", IEEE Transaction on Image Processing, vol. 22, no. 4, **(2013)**, pp. 1382-1394

[2] *Corresponding Author

[14] W. Dong, G. Shi and X. Li, "Nonlocal Image Restoration with Bilateral Variance Estimation: A Low-Rank Approach", IEEE Transactions on Image Processing, vol. 22, no. 2, **(2013)**, pp.700-711.
[15] G. Jeon, "Directionally Categorized Training Process for Hybrid Super-Resolution Algorithm", International Journal of Multimedia and Ubiquitous Engineering, vol. 9, no. 3, **(2014)**, pp. 107-116.
[16] W. T. Freeman and C. Liu, "Markov random fields for super- resolution and texture Synthesis", Advances in Markov Random Fields for Vision and Image Processing, Chapter 10.MIT Press, **(2011)**.
[17] R. Zeyde, M. Elad and M. Protter, "On single image scale-up using sparse-representations, Curves and Surfaces", Lecture Notes in Computer Science, vol. 6920, **(2012)**, pp. 711-730.
[18] H. Yu, F. Chen, Z. Zhang and C. Wang, "Single infrared image super-resolution combining non-local means with kernel regression", Infrared Physics & Technology, vol. 61, **(2013)**, pp. 50-59.
[19] Z. Gang, Z. Kai, S. Wei and Y. Jie, "A Study on NSCT based Super-Resolution Reconstruction for Infrared Image", TENCON 2013-2013 IEEE Region 10 Conference, **(2013)**, pp. 1-5.
[20] J. Wang, J. F. Ralph and J. Goulermas, "An Analysis of a Robust Super Resolution Algorithm for Infrared Imaging", Proceedings of 6th International Symposium on Image and Signal Processing and Analysis, Salzburg, **(2009)**, pp. 158-163.
[21] H. Liu, S. Li and H. Yin, "Infrared surveillance image super resolution via group sparse representation", Optics Communication, vol. 289, **(2013)**, pp. 45-52.
[22] M. Aharon, M. Eladan and A M. Bruckstein, "K-SVD: An Algorithm for Designing Over complete Dictionaries for Sparse Representation", IEEE Transactions on Signal Processing, vol. 54, no. 11, **(2006)**, pp. 4311-4233.
[23] M. N. Do and M. Vetterli, "The Contourlet Transform: An Efficient Directional Multiresolution Image Representation", IEEE Transactions on Image Processing, vol. 14, no. 12, **(2005)**, pp. 2091-2106.
[24] A. L. D. Cunha, J. Zhou and M. N. Do, "The Nonsubsampled Contourlet Transform: Theory, Design and Applications", IEEE Transaction on Image Processing, vol. 15, no. 10, **(2006)**, pp. 3089-3101.
[25] Q. Zhang and B. Guo, "Multifocus image fusion using the nonsubsampled contourlet transform", Signal Processing, vol. 89, no. 7, **(2009)**, pp. 1334-1346.
[26] H. Li, Y. Chai and Z. Li, "Multi-focus image fusion based on nonsubsampled contourlet transform and focus regions detection", Optik- International Journal for Light and Electron Optics, vol. 124, no. 1, **(2013)**, pp. 40-51.
[27] Y. Li, J. Hu and Y. Jia, "Automatic SAR image enhancement based on nonsubsampled contourlet transform and memetic algorithm", Neurocomputing, vol. 134, no. 25, **(2014)**, pp. 70-78.
[28] S. Yang, M. Wang, Y. X. Lu, W. Qi and L. Jiao, "Fusion of multiparametric SAR images based on SW-nonsubsampled contourlet and PCNN", Signal Processing, vol. 89, no. 12, **(2009)**, pp. 2596-2608.
[29] R. R. Sanchez, J. A. Garcia and J. F. Valdivia, "Image in painting with nonsubsampled contourlet transform", Pattern Recognition Letters, vol. 34, no. 13, **(2013)**, pp. 1508-1518.
[30] R. Rubinstein, M. Zibulevsky and M. Elad, "Double Sparsity: Learning Sparse Dictionaries for Sparse Signal Approximation", IEEE Transactions on Signal Processing, vol. 58, no. 3, **(2010)**, pp. 1553-1564.
[31] K. Engan, S. Aase, and J. Husoy, "Method of optimal directions for frame design", Proceedings of IEEE International Conference on Acoustics, Speech, and Signal Processing, Phoenix, AZ, vol. 5, **(1990)**, pp. 2443-2446.
[32] W. Wu and C. Zheng, "Single image super-resolution using self-similarity and generalized nonlocal mean", TENCON 2013-2013 IEEE Region 10 Conference, Xi'an, China, **(2013)**, pp. 1-4.
[33] Y. Zhang, W. Wu, Y. Dai, X. Yang, B. Yan and W. Lu, "Remote Sensing Image Super- resolution Based on Sparse Dictionaries and Residual Dictionaries", 2013 IEEE 11th International Conference on Dependable, Autonomic and Secure Computing, Chengdu, China, **(2013)**, pp. 318-323.
[34] S. Wang, Z. Liu, S. Lv, Y. Lv, G. Wu, P. Peng, F. Chen and X. Wang, "A Natural Visible and Infrared Facial Expression Database for Expression Recognition and Emotion Inference", IEEE Transactions on Multimedia, vol. 12, no. 7, **(2010)**, pp. 682-691.
[35] "flir.com(1999-2013)FLIR Systems,Inc", [Online]Available: http://www.cvs.flir.com/l/6132/2011-08-02/1ARLR?pi_ad_id=35322332185&gclid=COa2uNTZxccCFUEljgodZpQGTA.
[36] A. Burlacu and C. Lazar, "Image Feature Detection using Phase Congruency and Its Application in Visual Serving", 2008 IEEE 4th International Conference on Intelligent Computer Communication and Processing, Cluj-Napoca, **(2010)**, pp. 47-52.
[37] S. E. Grigoresu, N. Petkov and P. Kruizinga, "Comparison of Texture Features Based on Gabor Filters", IEEE Transaction on Image Processing, vol. 11, no. 10, **(2002)**, pp. 1160-1167.

Authors

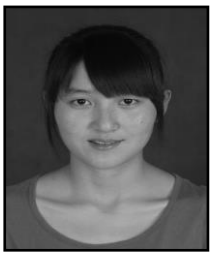

Kangli Li, received his BS degree of Information Engineering from Sina international University, China in 2012. Now she is a postgraduate in School of Electronics and Information Engineering, Sichuan University. Her research interests are image process, computer vision and pattern recognition.

Wei Wu, is currently an Associate Professor in College of Electronics and Information Engineering, Sichuan University, China. He received his BS degree from Tianjin University, China in 1998 and received his MS degree and PhD degrees in communication and information system from Sichuan University China in 2003 and 2008, respectively. He worked in a National Research Council Canada as a post-doctorate in 2009 - 2010. He has published over 50 scholarly papers in academic journals and conferences. He serves as an associate editor of Journal of Pattern Recognition Research. His research interests are image process, computer vision and pattern recognition.

Xiaomin Yang, is currently an Associate Professor in College of Electronics and Information Engineering, Sichuan University. She received her BS degree from Sichuan University, and received PhD degrees in communication and information system from Sichuan University. She worked in University of Adelaide as a post doctorate for one year. She has published over 30 scholarly papers in academic journals and conferences. Her research interests are image process and pattern recognition.

Yingying Zhang, received her BS degree from wenjing college, Yantai University, China, in 2011, and her MS degree in School of Electronics and Information Engineering, Sichuan University, in 2014. Her research interests are image process, computer vision.

Binyu Yan, is currently an Associate Professor in College of Electronics and Information Engineering, Sichuan University. He received his BS degree from Sichuan University, China in 1997, and received his MS and PhD degrees in communication and information system from Sichuan University.His research interests are image process and pattern recognition.

Wei Lu, is currently a Professor in School of Software Engineering, Beijing Jiaotong University, China. He received his BS degree from Liaoning Shihua University, China in 1985, received his MS degree in computer application from Sichuan University China in 1998, and received his PhD degrees communication and information system from Sichuan University China in 2006. His research interests are soft engineering and computer network.

Gwanggil Jeon, received the BS, MS, and PhD (summa cum laude) degrees in Department of Electronics and Computer Engineering from Hanyang University, Seoul, Korea, in 2003, 2005, and 2008, respectively. From 2008 to 2009, he was with the Department of Electronics and Computer Engineering, Hanyang University, from 2009 to 2011, he was University of Ottawa, as a postdoctoral fellow, and from 2011 to 2012, he was with the Graduate School of Science & Technology, Niigata University, as an assistant professor. He is currently an assistant professor with the Department of Embedded Systems Engineering, University of Incheon, Incheon, Korea. His research interests fall under the umbrella of image processing, particularly image compression, motion estimation, demosaicking, and image enhancement as well as computational intelligence such as fuzzy and rough sets theories. He was the recipient of the IEEE Chester Sall Award in 2007 and the 2008 ETRI Journal Paper Award.